PAPER

Mechanical stability of *cis*, *trans*-poly(*p*-phenylene vinylenes)†

Yurachat Janpatompong,‡ Kamil Suwada,‡ Michael L. Turner [ID] * and Guillaume De Bo [ID] *

Understanding the stability of conjugated polymers towards mechanical stimuli is critical for optimizing the processing and use of these materials in a range of electronic and optoelectronic devices, such as transistors, light emitting diodes and solar cells. The fast-growing field of mechanochemistry aims to tame the destructive mechanical forces to perform specific chemical changes in mechanophores but it can also be used to probe the stability of conjugated polymers towards destructive mechanical forces. Using ultrasonication it is possible to benchmark the mechanical integrity of phenylenevinylene block copolymers and show, through experimental studies and DFT simulation, that conjugated olefins are highly stable to *cis*–*trans* isomerisation upon extensive elongation, a useful property for the development of flexible organic electronics.

Introduction

π-Conjugated polymers have been processed from solution into the active layer of electronic devices such as organic light emitting diodes (OLEDs),[1–4] organic photovoltaics (OPVs)[5–8] and organic field-effect transistors (OFETs).[9–13] The performance of these devices is greatly influenced by the morphology of the active layer, and this is strongly influenced by the kinetics of thin film formation during device fabrication.[6,14,15] In addition, there is an increasing focus on printing or roll-to-roll processing of these materials to fabricate flexible light-weight devices over large areas.[16] Rod-coil block copolymers are of interest due to the possible long range order of the self-assembled thin film morphologies.[17–20] These significantly influence the optoelectronic properties of the conjugated polymer blocks and can dramatically affect the polymer solubility, crystallization, morphology, aggregation and self-assembly.[21,22]

Many modern consumer electronics are designed to be conformable, bent or flexed in use. This means that the individual components (*i.e.* transistors, diodes, resistors, capacitors) need to be mechanically robust to extension and flexing and the performance of these devices must be stable under repeated mechanical deformation.[23] Semiconducting polymers often do not exhibit the same mechanical strength and toughness of traditional engineering polymers as they have rigid planar backbones that are ordered in the solid state but are surrounded by long, flexible side chains to enhance solubility, reducing the cohesive forces within thin films of these materials.[24] Although the thickness of the active semiconducting layer of most flexible electronic devices is more than an order of magnitude less than that of other layers, mechanical change or damage within these layers leads to dramatic changes in device performance.[25] An understanding of the destructive nature of mechanical energy on the chemical structure of conjugated polymers will help in the design of materials for mechanically robust, functional devices.

Application of elongational force to organic molecules embedded in the polymer backbone can be achieved in solution using high intensity ultrasound (as solvodynamic shear is generated in the surrounding of collapsing cavitation bubbles).[26,27] This technique has been used to activate a variety of mechanophores,[28] sometimes along unusual reaction pathways,[29–31] prepare functional materials,[32] carry out *in situ* catalysis,[33,34] or induce the release of small molecules,[35] amongst others. Here we investigate the mechanical strength of *cis*, *trans*-poly(*p*-phenylene vinylenes) (PPVs) under tensional force. The mechanical activation was performed in solution using high-intensity ultrasound. We anticipated the possible *cis* to *trans* isomerisation of the olefins upon elongation, a phenomenon previously observed by AFM,[36,37] but we found that the structural integrity (notably the stereochemistry of the double bonds) and the optical properties are conserved upon mechanical activation. The origin of PPV mechanical strength was investigated computationally by DFT using the

Department of Chemistry, The University of Manchester, Oxford Road, Manchester, M13 9PL, UK. E-mail: michael.turner@manchester.ac.uk, guillaume.debo@manchester.ac.uk

‡These authors contributed equally.

Constrained Geometry Simulates External Force (CoGEF) technique.[28,38]

Results and discussion

Mechanical activation of polymers by ultrasonication requires that the polymer molecular weight is above a limiting value (M_{lim}) above which mechanochemical coupling is effective. In this work triblock copolymers were prepared with a central *cis, trans* PPV segment for mechanical activation linked to long PMMA chains to ensure that the molecular weight of the chains exceeded the M_{lim} to allow for mechanochemical coupling. This is known to be more than 30 kDa for PMMA.[39] The preparation of the *cis, trans* PPV block was achieved *via* ROMP of substituted paracyclophanediene monomers **1** and **2** (Scheme 1).[21] The target length for the PPV block was 10 monomeric units and it was capped at both ends by an α-bromoester functional group. The macroinitiators **5** and **6** were used to grow PMMA blocks from both ends using ATRP. The ROMP process gives alternating *cis, trans* stereochemistry polymers due to the ring opening of only one vinylene of the cyclophanediene monomer (**1**, **2**) and the choice of cyclophanediene (**1** or **2**) enables the optoelectronic properties of these triblock copolymers to be modified.

Incorporation of the α-bromoester end group in **5** and **6** was achieved by quenching the living ROMP of cyclophanediene **1** and **2** with 20 eq. of vinyl ether *E/Z*-**4** (*f* = 96% and 76%) (Scheme 1). Polymers **5** and **6** were isolated as yellow solids after purification, in yields of 95 and 97%, respectively. The

presence of the α-bromoester end groups in polymers **5** and **6** enable these polymers to be used as macroinitiators in ATRP. The PMMA–PPV–PMMA triblock copolymers **7a** and **8a** were prepared by copper-catalyzed ATRP of MMA at 90 °C.[21,40] High molecular weight PMMA segments (Scheme 1) were obtained after heating for 16 and 15 hours, respectively. The polymerization was terminated by exposure of the reaction to air and the polymeric products were isolated by precipitation into methanol, followed by reprecipitation into diethyl ether from chloroform.

The molecular weights of **7a** and **8a** were determined by size exclusion chromatography (Table 1) in THF, calibrated using polystyrene standards. The number average molar masses (M_n) determined by SEC were 64.3 ($Đ = 1.40$) and 79.3 kDa ($Đ = 1.41$) for **7a** and **8a**, respectively. The ^{1}H NMR spectra of triblock copolymers **7a** and **8a** are shown in Fig. S5–8.† Resonances relating to PPV and PMMA segments are apparent, with the key signals assigned for each block. The resonances below 2.00 ppm are associated with the 2-(*R/S*) ethylhexyl and alkyl side chain and the C–CH$_3$ and CH$_2$ of the PMMA segment. An approximate degree of polymerization for the PMMA segment was calculated by integration of the OMe group of MMA ($\delta = 3.17$–3.98 ppm) against the combined phenyl and vinylene protons for **7a** ($\delta = 6.40$–7.53 ppm) and methylene protons for **8a** ($\delta = 2.16$–2.86 ppm) respectively. The degree of polymerization of the PMMA segment determined by ^{1}H NMR spectroscopy allowed for an absolute M_n value to be calculated (see Table 1). The discrepancy between the apparent M_n from SEC and the absolute M_n calculated from ^{1}H NMR spectroscopy is due to the difference in hydrodynamic volume between the triblock copolymer and the PS standards.[41]

Mechanochemical activation of the polymers **7a** and **8a** was performed by ultrasonication (20 kHz, 15.6 W cm^{-2}, 1 s on/2 s off) of dilute (~2 mg mL^{-1}) polymer solutions in the dark, while maintaining the temperature between 5 and 10 °C. The complete cleavage of both polymers was observed after 120 min of sonication (Fig. 1a, $M_n = 25.1$ and 25.7 kDa for **7b** and **8b** respectively). This transformation was indicative of the destructive mechanical forces acting on the triblock copolymer backbone, resulting in covalent bond scissions in the PMMA blocks. Despite the broad dispersity of polymers **7a** and **8a** ($Đ$ ~1.4), the PPV block should be placed in the central region of
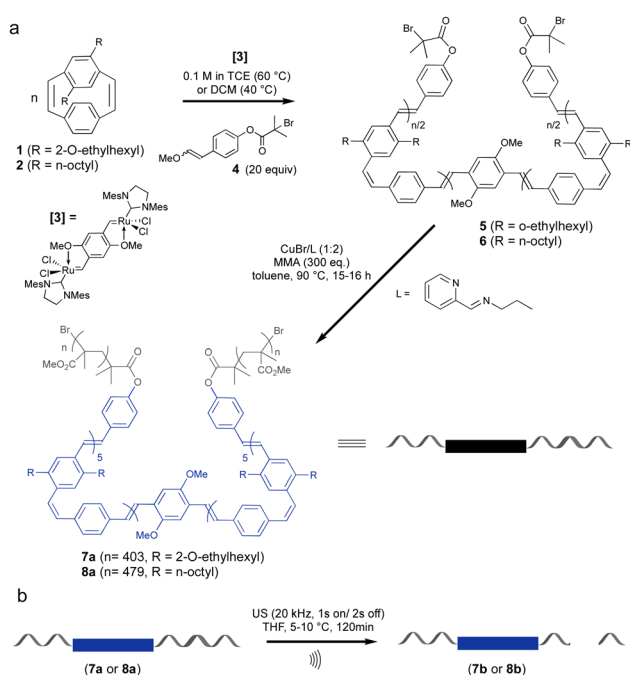
Scheme 1 Synthesis (a) and mechanical activation (b) of coil–rod–coil ABA phenylene-vinylene triblock copolymers **7a** and **8a**.

Table 1 Structural and optical data of the investigated polymers

	x_n (PPV)[a]	x_n (PMMA)[b]	$M_n{}^c$ (kg mol^{-1})	$Đ^c$	$M_n{}^b$ (kg mol^{-1})	λ_{max} (nm)	λ_{em} (nm)
5	—	—	5.86	1.24	5.19	451	527
6	—	—	6.24	1.32	4.72	382	495
7a	10	806	64.31	1.40	85.85	452	528
7b	10	806	25.08	1.42	—	452	528
8a	10	958	79.30	1.41	100.55	374	493
8b	10	960	25.69	1.34	—	374	493

[a] From [**5**]/[catalyst **3**] or [**6**]/[catalyst **3**]. [b] Determined by ^{1}H NMR spectroscopy. [c] Determined by SEC with RI detection (calibrated against narrow $Đ$ PS standards).
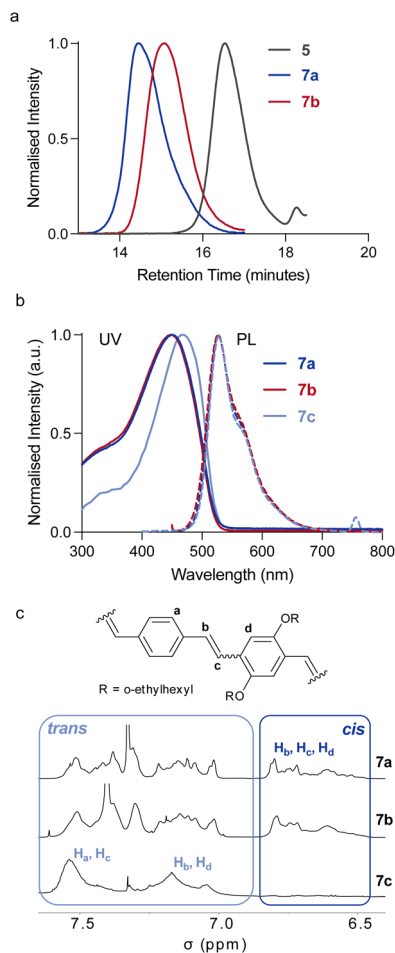
Fig. 1 SEC traces (a), UV-PL spectra (b), and partial ^{1}H NMR spectra (500 MHz, CD_2Cl_2) (c) of pre- and post-sonication polymers **7a** and **7b** respectively, along with all-*trans* reference polymer **7c**. Spectra aligned on the $-OCH_3$ peak of PMMA.

Fig. 2 Structure of **7′** used for CoGEF simulations with constrained atoms marked in bold and scissile bond highlighted in red (a), along with its energy minimized structure (b). The evolution of energy upon simulated elongation (CoGEF, DFT B3LYP/6-31G*) of this model (c) reveals the most elongated (E_{max}) and post-scission structures (d).

Fig. 3 Changes in selected angles (plain) and dihedrals (dashed) upon simulated elongation of **7′**.

the block copolymer in most of the chains. In any case, as force is distributed along the backbone (with its highest intensity in the centre), it is possible to activate a mechanophore that is located off-centre,[42,43] especially for a low-force process such as olefin isomerisation (which typically occur ~1 nN).[36,37]

The ^{1}H NMR spectra of **7a,b** and **8a,b** pre- and post-sonication showed no substantional changes in the olefin signals (Fig. 1c and Fig. S5–8†), indicating that no *cis, trans* isomerisation occurred in the PPV block during sonication. This was also confirmed by the absorption and emission spectra of rod–coil triblock copolymer **7** (Fig. 1b), which show no difference between pre- and post-sonication samples (**7a** and **7b**). The UV-vis spectrum exhibits a λ_{max} of 452 nm, with a PL_{max} at 528 nm while polymer **8** shows a λ_{max} of 374 nm and a PL_{max} at 493 which is blue shifted from **7** (Table 1).

As the mechanical elongation led to polymer backbone degradation before chemical changes could occur at the PPV block, the scission very likely occurred within the PMMA backbone. To gain better understanding of the PPV moiety under stress, calculations were performed on models of polymers **7a**
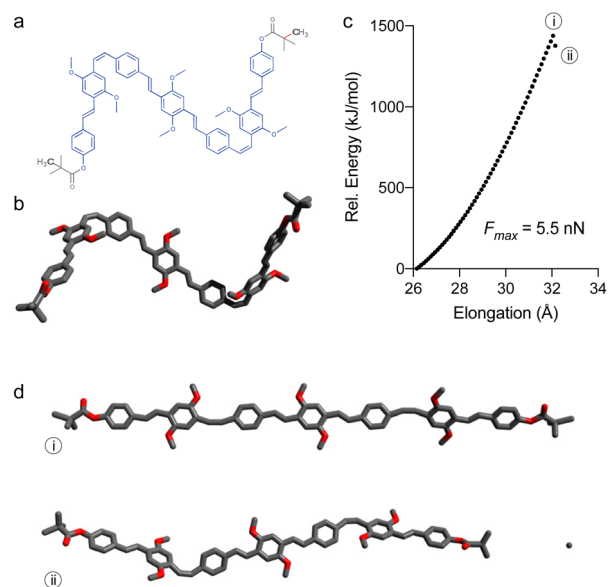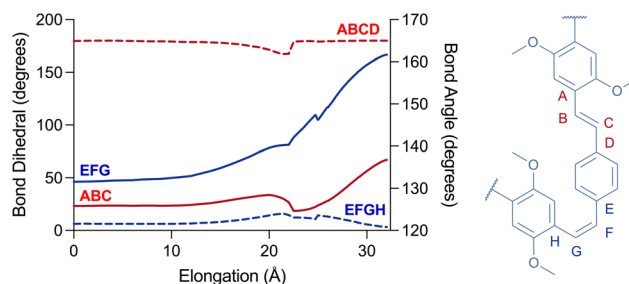
(Fig. 2 and 3) and **8a** (Fig. S1†), which were constructed from the initiator and one ROMP monomer unit on each side, capped by pivalate moiety simulating the PMMA attachment point (**7′** and **8′**, respectively). The elongation of these models was simulated by incrementally increasing the distance between the anchor atoms and optimizing the geometry at each step (CoGEF, DFT B3LYP 6-31G$^+$ (d′, 3p′) level of theory in Gaussian 16). Both models experience a high degree of deformation upon simulated elongation before the scission of a terminal bond is observed (Fig. 2c), which is indicative of a non-selective scission within PMMA block. Both **7′** and **8′** show a similar F_{max} value of 5.5 nN (Fig. 2c and S1†), while CoGEF simulation of a PPV segment derived from **7′** (*i.e.* without pivalate groups, see ESI†) leads to the scission of the C–C bond separating the *cis*-olefin from the substituent-free ring at a considerably higher force of 6.9 nN, which is beyond the force required to cleave the PMMA backbone (see ESI†).

Remarkably, no isomerisation takes place during the elongation (Fig. 3). Instead, the simulated force led to the distortion of *trans*-olefins from 129° up to 140° (angle ABC), while the *cis*-olefins have bent from 131° to nearly 162° (angle EFG) at E_{max} (i, Fig. 2c and d) for 7′. Moreover, the ring-adjacent bonds (*e.g.* AB) elongated from ~1.46 Å to as high as 1.65 Å, while the vinylene bonds (*e.g.* BC) elongated from ~1.35 Å up to 1.44 Å. Unsurprisingly, the *cis*-olefins experienced a higher level of distortion than the *trans*-isomers. The rings themselves experience a lower deformation as cross-ring distance D–E elongates from 2.86 Å up to 3.09 Å for example. Taken together these observations explain why the PPV polymers do not isomerise during stretching, as the elongational force applied during sonication does not provide the torsional momentum (*i.e.* the opening of dihedral angle EFGH) required to flip the olefins from *Z* to *E* stereochemistry.

Conclusions

The mechanical stability of *cis*, *trans*-PPVs was investigated in solution by sonicating PMMA–PPV–PMMA triblock copolymers. The mechanical stress induced by the sonication led to the scission of the PMMA blocks instead of isomerisation or scission of the central conjugated fragment. Despite the effectively higher elongational forces acting on the conjugated segment of the triblock chain, this PPV block maintained its initial photophysical properties as no bond scission or isomerisation occurred. Computational simulation of the elongation process using the CoGEF technique reveals that the elongational force applied during sonication did not provide the torsional momentum required for the isomerisation of olefins. The results bode well for the development of flexible organic electronics utilising PPVs and using mechanochemistry to benchmark stability of conjugated polymers in general.

Conflicts of interest

There are no conflicts to declare.

Acknowledgements

References

1 M. Gross, D. C. Müller, H.-G. Nothofer, U. Scherf, D. Neher, C. Bräuchle and K. Meerholz, *Nature*, 2000, **405**, 661–665.

2 Y. Liu, S. Yan and Z. Ren, *Chem. Eng. J.*, 2021, **417**, 128089.

3 W. Lu, J. Kuwabara, T. Iijima, H. Higashimura, H. Hayashi and T. Kanbara, *Macromolecules*, 2012, **45**, 4128–4133.

4 R. M. Pankow and B. C. Thompson, *Polymer*, 2020, **207**, 122874.

5 X. Zhan and D. Zhu, *Polym. Chem.*, 2010, **1**, 409–419.

6 B. Zheng, L. Huo and Y. Li, *NPG Asia Mater.*, 2020, **12**, 3.

7 Y. Xu, Y. Cui, H. Yao, T. Zhang, J. Zhang, L. Ma, J. Wang, Z. Wei and J. Hou, *Adv. Mater.*, 2021, **33**, 2101090.

8 J.-H. Kim, S. Wood, J. B. Park, J. Wade, M. Song, S. C. Yoon, I. H. Jung, J.-S. Kim and D.-H. Hwang, *Adv. Funct. Mater.*, 2016, **26**, 1517–1525.

9 J. Yang, Z. Zhao, S. Wang, Y. Guo and Y. Liu, *Chem*, 2018, **4**, 2748–2785.

10 S. Nagasawa, E. Al-Naamani and A. Saeki, *J. Phys. Chem. Lett.*, 2018, **9**, 2639–2646.

11 S. Choi, J. W. Jeong, G. Jo, B. C. Ma and M. Chang, *Nanoscale*, 2019, **11**, 10004–10016.

12 M. Pandey, N. Kumari, S. Nagamatsu and S. S. Pandey, *J. Mater. Chem. C*, 2019, **7**, 13323–13351.

13 R. Zhao, Y. Min, C. Dou, B. Lin, W. Ma, J. Liu and L. Wang, *ACS Appl. Polym. Mater.*, 2020, **2**, 19–25.

14 K. Weng, L. Ye, L. Zhu, J. Xu, J. Zhou, X. Feng, G. Lu, S. Tan, F. Liu and Y. Sun, *Nat. Commun.*, 2020, **11**, 2855.

15 M. D. M. Faure and B. H. Lessard, *J. Mater. Chem. C*, 2021, **9**, 14–40.

16 K. Liu, B. Ouyang, X. Guo, Y. Guo and Y. Liu, *npj Flexible Electron.*, 2022, **6**, 1–19.

17 M. He, F. Qiu and Z. Lin, *J. Mater. Chem.*, 2011, **21**, 17039–17048.

18 Y. Tao, B. Ma and R. A. Segalman, *Macromolecules*, 2008, **41**, 7152–7159.

19 P. D. Topham, A. J. Parnell and R. C. Hiorns, *J. Polym. Sci., Part B: Polym. Phys.*, 2011, **49**, 1131–1156.

20 Y.-C. Chiu, C.-C. Shih and W.-C. Chen, *J. Mater. Chem. C*, 2015, **3**, 551–558.

21 V. Komanduri, D. R. Kumar, D. J. Tate, R. Marcial-Hernandez, B. J. Lidster and M. L. Turner, *Polym. Chem.*, 2019, **10**, 3497–3502.

22 D.-H. Jiang, B. J. Ree, T. Isono, X.-C. Xia, L.-C. Hsu, S. Kobayashi, K. H. Ngoi, W.-C. Chen, C.-C. Jao, L. Veeramuthu, T. Satoh, S. H. Tung and C.-C. Kuo, *Chem. Eng. J.*, 2021, **418**, 129421.

23 J. P. Cachaneski-Lopes and A. Batagin-Neto, *Polymers*, 2022, **14**, 1354.

24 S. E. Root, S. Savagatrup, A. D. Printz, D. Rodriquez and D. J. Lipomi, *Chem. Rev.*, 2017, **117**, 6467–6499.

25 M. Brinkmann, L. Hartmann, L. Biniek, K. Tremel and N. Kayunkid, *Macromol. Rapid Commun.*, 2014, **35**, 9–26.

26 G. De Bo, *Macromolecules*, 2020, **53**, 7615–7617.

27 P. A. May and J. S. Moore, *Chem. Soc. Rev.*, 2013, **42**, 7497–7506.

28 I. M. Klein, C. C. Husic, D. P. Kovács, N. J. Choquette and M. J. Robb, *J. Am. Chem. Soc.*, 2020, **142**, 16364–16381.

29 R. Nixon and G. De Bo, *Nat. Chem.*, 2020, **12**, 826–831.

30 Y. Liu, S. Holm, J. Meisner, Y. Jia, Q. Wu, T. J. Woods, T. J. Martinez and J. S. Moore, *Science*, 2021, **373**, 208–212.

31 J. M. Lenhardt, M. T. Ong, R. Choe, C. R. Evenhuis, T. J. Martinez and S. L. Craig, *Science*, 2010, **329**, 1057–1060.

32 Z. Chen, J. A. M. Mercer, X. Zhu, J. A. H. Romaniuk, R. Pfattner, L. Cegelski, T. J. Martinez, N. Z. Burns and Y. Xia, *Science*, 2017, **357**, 475–479.

33 A. Piermattei, S. Karthikeyan and R. P. Sijbesma, *Nat. Chem.*, 2009, **1**, 133–137.

34 P. Michael and W. H. Binder, *Angew. Chem., Int. Ed.*, 2015, **54**, 13918–13922.

35 R. Küng, R. Göstl and B. M. Schmidt, *Chem. – Eur. J.*, 2022, **28**, e202103860.

36 W. Huang, Z. Zhu, J. Wen, X. Wang, M. Qin, Y. Cao, H. Ma and W. Wang, *ACS Nano*, 2017, **11**, 194–203.

37 M. Radiom, P. Kong, P. Maroni, M. Schäfer, A. F. M. Kilbinger and M. Borkovec, *Phys. Chem. Chem. Phys.*, 2016, **18**, 31202–31210.

38 M. K. Beyer, *J. Chem. Phys.*, 2000, **112**, 7307–7312.

39 M. M. Caruso, D. A. Davis, Q. Shen, S. A. Odom, N. R. Sottos, S. R. White and J. S. Moore, *Chem. Rev.*, 2009, **109**, 5755–5798.

40 B. J. Lidster, J. M. Behrendt and M. L. Turner, *Chem. Commun.*, 2014, **50**, 11867–11870.

41 L. Jones, D. L. Pearson, J. S. Schumm and J. M. Tour, *Pure Appl. Chem.*, 1996, **68**, 145–148.

42 K. L. Berkowski, S. L. Potisek, C. R. Hickenboth and J. S. Moore, *Macromolecules*, 2005, **38**, 8975–8978.

43 J. M. Lenhardt, A. L. Black Ramirez, B. Lee, T. B. Kouznetsova and S. L. Craig, *Macromolecules*, 2015, **48**, 6396–6403.